JACS
JOURNAL OF THE AMERICAN CHEMICAL SOCIETY
Communication
pubs.acs.org/JACS

Exceptionally Long-Lived Charge Separated State in Zeolitic Imidazolate Framework: Implication for Photocatalytic Applications

Brian Pattengale,[†] Sizhuo Yang,[†] John Ludwig,[†] Zhuangqun Huang,[†] Xiaoyi Zhang,[‡] and Jier Huang*,[†]

[†]Department of Chemistry, Marquette University, Milwaukee, Wisconsin 53201, United States
[‡]X-ray Science Division, Argonne National Laboratory, Argonne, Illinois 60349, United States

Supporting Information

ABSTRACT: Zeolitic imidazolate frameworks (ZIFs) have emerged as a novel class of porous metal−organic frameworks (MOFs) for catalysis application because of their exceptional thermal and chemical stability. Inspired by the broad absorption of ZIF-67 in UV−vis-near IR region, we explored its excited state and charge separation dynamics, properties essential for photocatalytic applications, using optical (OTA) and X-ray transient absorption (XTA) spectroscopy. OTA results show that an exceptionally long-lived excited state is formed after photoexcitation. This long-lived excited state was confirmed to be the charge-separated (CS) state with ligand-to-metal charge-transfer character using XTA. The surprisingly long-lived CS state, together with its intrinsic hybrid nature, all point to its potential application in heterogeneous photocatalysis and energy conversion.

Zeolitic imidazolate frameworks (ZIFs) represent an emerging subclass of metal organic frameworks (MOFs) constructed from tetrahedral coordinated transition-metal cations (M) bridged by imidazole-based ligands (Im).[1,2] Because the M−Im−M angle in ZIF (~145°) is similar to Si−O−Si angle in conventional silicon-based zeolites, ZIFs give rise to zeolite-type topology. Unlike zeolite, ZIFs are unique in structural flexibility including tunable framework, pore aperture, and surface area.[1,2] Indeed, over 150 ZIF structures have, to date, been synthesized, many of which are microporous with inherently large surface areas and tunable cavities, and exhibit exceptional thermal and chemical stability.[3−6] Thus, ZIFs demonstrate great promise in various applications such as gas separation and storage,[6−11] chemical sensing,[12] and heterogeneous catalysis.[13−17]

Driven by the increasing global energy demand, recent development in the field has extended the application of ZIF materials toward photocatalysis using visible light. Although still in the early stage of exploration, ZIFs have been used as photocatalysts for dye and phenol degradation as well as CO_2 reduction.[15,17−19] In these systems, photoactive nanostructures/molecules are incorporated into the highly porous structure of ZIFs, where ZIFs are used as a simple host or passive medium for dispersing the catalytic active species. This strategy has been widely used in developing zeolite-based photocatalysts[20] and recently in preparing MOF/nanocomposite or MOF/molecular catalyst hybrids,[19,21,22] yet suffers from challenges, notably the difficulty in preventing the guest material aggregation and the lack of the control over spatial distribution and homogeneity.[21,23−26] An alternative approach, which has recently been used in developing photoactive MOFs, is to develop the framework which exhibits an intrinsic photochemical response and thereby can be directly applied in photocatalysis.[27,28]

As photocatalysis is based on a charge-transfer (CT) event following photoexcitation, it is essential to gain an intimate knowledge of the excited-state and charge transport properties within the ZIF framework, the properties that remain unexplored. Here, we report the first study on the excited-state dynamics in ZIF-67 thin film using optical transient (OTA) and X-ray transient absorption (XTA) spectroscopy. We show that charge separation (CS) occurs in the framework of ZIF-67 by forming a superlong intermediate state with ligand-to-metal charge-transfer (LMCT) character.

ZIF-67 thin film was synthesized according to the established synthetic protocols.[29] The details of the synthesis of ZIF-67 are described in Supporting Information (SI). The morphology of the ZIF-67 film was characterized by atomic force microscopy (AFM) in the PeakForce feedback mode. As shown in Figure 1a,b, the synthesized ZIF-67 film is continuous and consists of crystals with truncated rhombic dodecahedral shape with ~300−500 nm size. The cross-section views of the film (Figure S1) indicate that the thickness of the film is ~350 nm, suggesting that the film is likely composed of single crystal layer.

The bulk structure of ZIF-67 was measured by powder X-ray diffraction (XRD). As shown in Figure 1c, XRD patterns obtained for the synthesized sample agree well with the peaks characteristic of ZIF-67,[30] suggesting the successful synthesis of ZIF-67. Furthermore, the local structure of ZIF-67 at Co center was examined using steady-state X-ray absorption spectroscopy (XAS). Figure 1d shows the X-ray absorption near edge structure (XANES) spectrum of ZIF-67 at Co K-edge. The XANES spectrum of $Co(NO_3)_2{\cdot}6H_2O$,which is the starting material known for octahedral (O_h) coordination at Co center, is also shown in Figure 1d for comparison. The prominent pre-edge feature (quadrupole allowed 1s−3d transition) in ZIF-67, characteristic of tetrahedral (T_d) coordination,[31,32] is distinct from the negligible 1s−3d transition in the O_h coordinated $Co(NO_3)_2{\cdot}6H_2O$. Furthermore, the main absorption edge in the XANES spectrum of ZIF-67, arising from dipole allowed 1s−4p transition, shows a less sharp peak than that of $Co(NO_3)_2{\cdot}6H_2O$, which can be ascribed to the decreased multiple scattering for a T_d coordination in the former compared with O_h geometry in the

Received: May 4, 2016
Published: June 20, 2016

DOI: 10.1021/jacs.6b04615
J. Am. Chem. Soc. 2016, 138, 8072−8075

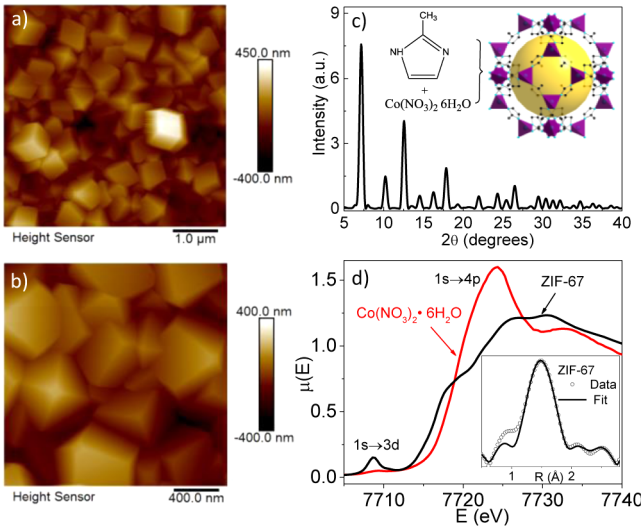

Figure 1. (a and b) AFM topography images of ZIF-67 thin film. (c) Powder XRD patterns of ZIF-67. The inset shows the synthetic scheme for the formation of ZIF-67 crystal. The yellow ball indicates the cavity in the framework. (d) XANES spectra of ZIF-67 and $Co(NO_3)_2{\cdot}6H_2O$. The inset shows the XAFS spectrum and its fitting in R-space.

latter.[32] The T_d structure is further confirmed by quantitatively analyzing the extended X-ray absorption fine structure (EXAFS) spectrum (inset of Figure 1d and Figure S2), which clearly demonstrates that Co has four nitrogen neighbors with the average distance of Co−N 1.99 ± 0.02 Å.

Figure 2a shows the UV−vis-near IR absorption spectrum of ZIF-67 film. The spectrum exhibits three absorption features,

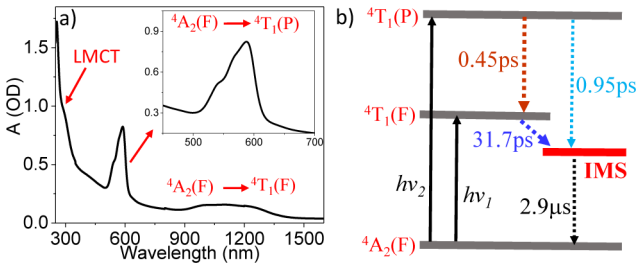

Figure 2. (a) UV−vis-near IR absorption spectrum of ZIF-67 thin film. (b) The schematic representation of energy diagram of Co^{2+} (T_d) and excited-state relaxation of ZIF-67.

including a broad absorption in UV region (<400 nm), a visible band with three maxima centered at 588, 567, and 539 nm (inset of Figure 2a), and a broad near IR band from 900 to 1400 nm. These features can be attributed to the LMCT transition, the higher-lying [$^4A_2(F)-{}^4T_1(P)$] and lower-lying [$^4A_2(F)-{}^4T_1(F)$] d−d ligand field transitions (Figure 2b), respectively, and are well-known features for Co^{2+} ion in T_d environment,[33,34] consistent with the above XRD and XAS results.

Ultrafast OTA spectroscopy was used to investigate the excited-state dynamics of ZIF-67 by selectively exciting the two d−d transitions. Figure 3a shows the femtosecond OTA (fs-OTA) spectra of ZIF-67 thin film in the visible region after exciting the lower-lying d−d band using 1000 nm light. Immediately following excitation, the OTA spectrum shows a negative band with triplet maximum in 520−600 nm region and a broad positive feature at >605 nm. The negative band strongly resembles the inverted ground-state (GS) absorption of

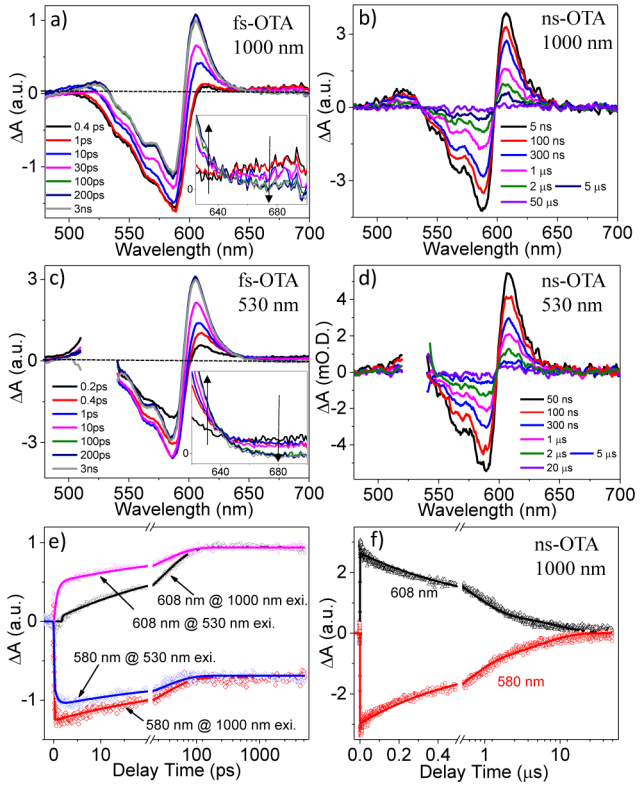

Figure 3. Femtosecond (a) and nanosecond (b) OTA spectra of ZIF-67 after 1000 nm excitation. Femtosecond (c) and nanosecond (d) OTA spectra of ZIF-67 after 530 nm excitation. (e) The kinetics at 608 and 580 nm in femtosecond OTA spectra of ZIF-67 after 1000 and 530 nm excitation. (f) The kinetics at 608 and 580 nm in nanosecond OTA spectra of ZIF-67 after 1000 nm excitation.

$^4A_2(F)-{}^4T_1(P)$ transition and can thus be attributed to the bleach of $^4A_2(F)$ state due to photoexcitation. The broad positive band decays within ∼200 ps (inset of Figure 3a), which is accompanied by the emergence of a new positive band centered at 605 nm. These two features are separated by a clear isosbestic point at 647 nm, suggesting that the decay of the former is associated with the formation of the latter. Meanwhile, another positive band was formed at ∼525 nm within the same time regime. All of these spectral features together made the whole OTA spectra derivative-like shape, which maintains through the microsecond time as shown in nanosecond OTA (ns-OTA) spectra (Figure 3b), where the recovery of GS bleach and the decay of the two absorption bands centered 525 and 605 nm occur simultaneously. The presence of two isosbestic points at 536 and 599 nm confirms that these spectral evolutions are associated with the same recombination process. Similar spectral features were also observed in the near-IR OTA spectra representing the $^4A_2(F)-{}^4T_1(F)$ transition (Figure S3), consistent with our assignment earlier that the two d−d bands share the same GS, i.e., $^4A_2(F)$.

Upon excitation of the higher-lying d−d band using 530 nm light, both fs- (Figure 3c) and ns-OTA spectra (Figure 3d) show the similar spectral features as the spectra after 1000 nm excitation, i.e., the instantly formed GS bleach and broad absorption (>605 nm) which decays to form a long-lived intermediate state with derivative-like spectral feature. However, extra rising components were observed in both GS bleach and 605 nm absorption band in the spectra of 530 nm excitation. These additional features can be more clearly seen in Figure 3e,

DOI: 10.1021/jacs.6b04615
J. Am. Chem. Soc. 2016, 138, 8072−8075

Table 1. Fitting Parameters for fs- and ns-OTA Results

pump (nm)	probe (nm)	τ_1, ps (A_1,%)	τ_2, ps (A_2,%)	τ_3, μs (A_3,%)	τ_4, μs (A_4,%)
1000	608	31.7 (100)[a]		0.64 (74.2)	9.2 (25.8)
	580	31.7 (43.3)		0.64 (42.1)	9.2 (14.6)
530	608	31.7 (46.2)[a]	0.95 (53.8)[a]	0.64 (74.2)	9.2 (25.8)
	580	31.7 (35.5)	0.45 (100)[a]	0.64 (47.9)	9.2 (16.6)

[a]The rising component.

where the kinetic traces at 580 and 608 nm after 530 and 1000 nm excitation were compared.

Given the interpretation of the OTA spectra above, we can assign the transient species to each specific process according to the model proposed in Figure 2b. The 1000 nm excitation ($h\upsilon_1$) depletes the $^4A_2(F)$ state accounting for the GS bleach in 520−600 and 900−1300 nm regions and populates $^4T_1(F)$ excited state accounting for the instantly formed broad absorption at >605 nm. The latter can be assigned to the photoinduced absorption of $^4T_1(F)$ state, which quickly decays to form the long-lived intermediate state (IMS) featured by the absorption bands centered at 525 and 605 nm. The kinetic traces at 580 and 608 nm in fs-OTA spectra can be fitted using biexponential functions, from which we obtained a short decay (580 nm) and rising (608 nm) component with 31.7 ps and a ultraslow decay component with ≫5 ns (Table 1). The 31.7 ps time constant can be assigned to the formation time of the IMS (Figure 2b). The ultraslow decay component can be accurately determined after fitting the ns-OTA kinetics (Figure 3f), from which we obtained two time constants of 0.64 μs (74.2%) and 9.2 μs (25.8%). The obtained amplitude weighted average time is 2.9 μs, suggesting the superlong lifetime of this IMS.

The kinetic traces at 580 and 608 nm in fs-OTA spectra after 530 nm excitation can be fitted using the same set of time constants above plus an additional rising component in each case (τ_2, Table 1). Because 530 and 1000 nm light excites Co^{2+} center from the same $^4A_2(F)$ to two different excited states, i.e., $^4T_1(P)$ and $^4T_1(F)$, respectively, we attribute the extra rising component (0.45 ps) at GS bleach of 530 nm excitation spectra to the relaxation process from $^4T_1(P)$ to $^4T_1(F)$, while the additional 0.95 ps time constant used in 608 nm kinetics to the formation of IMS directly from $^4T_1(P)$ state (Figure 2b). The ns-OTA kinetics after 530 nm excitation (Figure S4) can be adequately fitted using the same exponential function used in 1000 nm excitation, which further supports the formation of the same long-lived IMS regardless of the excitation of different d−d transitions.

It is interesting to note that the OTA spectra of the long-lived IMS closely match the second derivative of the GS absorption band (Figure S5). The derivative-like features have been observed in inorganic and organic semiconductors and are typically attributed to the presence of local fields due to the photoinduced electron−hole separation, which modifies the optical spectra due to the Stark effect.[35,36] The derivative-like spectral feature, along with extremely long lifetime of IMS, implies that the final IMS formed in ZIF-67 film after photoexcitation might be a charge-separated (CS) state rather than a metal centered state. To test this hypothesis and identify the nature of this IMS, we used XTA, a powerful technique in capturing the intermediate electronic structure at a specific metal center,[37−39] to probe the IMS electronic structure at Co center.

Figure 4a shows the XANES spectra of ZIF-67 before (laser-off) and after 527 nm excitation (laser-on) as well as the difference spectrum (blue curve) obtained after subtracting the laser-off spectrum from the laser-on spectrum. The laser-on

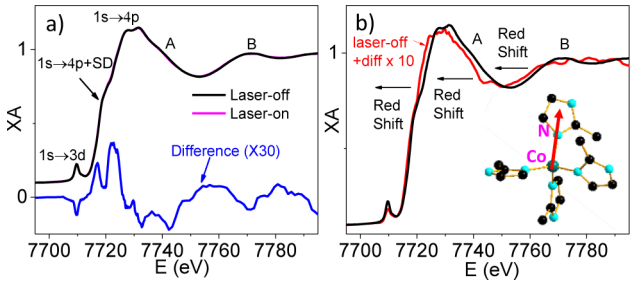

Figure 4. (a) XANES spectrum of ZIF-67 at Co K-edge before (laser-off) and 500 ps after (laser-on) laser excitation. The difference spectrum is obtained by subtracting the laser-off spectrum from laser-on spectrum. (b) To better illustrate the spectral change, the laser-on XANES spectrum is regenerated after adding the difference spectrum (× 10) to laser-off spectrum.

spectrum was taken at 500 ps after laser pump pulse when IMS has completely formed according to the OTA results. Therefore, any transient signal observed at this time delay is directly correlated with the IMS electronic structure. As shown in the difference spectrum in Figure 4a, a broad positive transient absorption was observed at white-line region (7714.9−7725.3 eV) where 1s−4p shake-down[40] and 1s−4p transition[41] occurs, indicating that the edge of Co center shifts to lower energy and hence the reduction of Co center due to photoexcitation. Because Co atom and imidazolate ligand are the only two components in ZIF-67, the reduction of Co center must be accompanied by the oxidation of the ligand, which unambiguously confirm the formation of CS state with LMCT character. The LMCT nature of the IMS is further supported by the negative feature at 7709.7 eV, corresponding to the reduced intensity of pre-edge (1s−3d) transition,[32,41] where the photoinduced charge separation by LMCT reduces the number of unoccupied Co 3d orbitals and hence the possibility of 1s−3d transition.

In addition to the transient signals at white-line and pre-edge regions, noticeable spectral changes were also observed at higher energy region (A and B in Figure 4). Feature A corresponds to multiple scattering processes. Feature B peaked around 7772 eV mainly comes from the single-scattering of the outgoing photoelectron from the nearest N atoms. To better illustrate the spectral changes in this region, we generated a new laser-on spectrum by adding the difference spectrum (× 10) to the laser-off spectrum. As shown in Figure 4b, clear red-shift is observed for B band in the laser-on spectrum (red plot) compared to the laser-off spectrum (black plot), which indicates the Co−N bond elongation after photoexcitation.

In summary, we examined the excited state and CS dynamics in ZIF-67 thin film using the combination of ultrafast OTA and XTA spectroscopy. OTA results clearly demonstrate the formation of an exceptionally long-lived IMS (~2.9 μs) within picosecond time scale after the photoexcitation of the spin-allowed d−d transition of Co^{2+} ion in ZIF-67. Using powerful

DOI: 10.1021/jacs.6b04615
J. Am. Chem. Soc. 2016, 138, 8072−8075

element specific XTA spectroscopy, this IMS was unambiguously confirmed to be the CS state with LMCT character. The unusually long-lived CS state and the broad absorption in UV–vis-near IR region, along with its hybrid porous nature, strongly imply the potential application of ZIF-67 materials in photocatalysis and energy conversion. Future work on understanding the localization/delocalization properties of this long-lived CS state in ZIF-67 framework is essential to facilitate these applications, which is currently ongoing in the group.

■ ASSOCIATED CONTENT

Supporting Information

The Supporting Information is available free of charge on the ACS Publications website at DOI: 10.1021/jacs.6b04615.

Experimental details and data (PDF)

■ AUTHOR INFORMATION

Corresponding Author

*jier.huang@marquette.edu

Notes

The authors declare no competing financial interest.

■ ACKNOWLEDGMENTS

This work was supported by Marquette University New Faculty Startup Fund and Regular Research Grant. Use of the Advanced Photon Source and nanosecond and femtosecond-NIR transient absorption spectroscopy at the Center for Nanoscale Materials in Argonne National Laboratory was supported by the U.S. Department of Energy, Office of Science, Office of Basic Energy Sciences, under award no. DE-AC02-06CH11357. Z.H. acknowledges help with AFM measurements from the Molecular Materials Research Center of the Beckman Institute, California Institute of Technology.

■ REFERENCES

(1) Phan, A.; Doonan, C. J.; Uribe-Romo, F. J.; Knobler, C. B.; O'Keeffe, M.; Yaghi, O. M. *Acc. Chem. Res.* **2010**, *43*, 58.

(2) Pimentel, B. R.; Parulkar, A.; Zhou, E. K.; Brunelli, N. A.; Lively, R. P. *ChemSusChem* **2014**, *7*, 3202.

(3) Moggach, S. A.; Bennett, T. D.; Cheetham, A. K. *Angew. Chem., Int. Ed.* **2009**, *48*, 7087.

(4) Fairen-Jimenez, D.; Moggach, S. A.; Wharmby, M. T.; Wright, P. A.; Parsons, S.; Duren, T. *J. Am. Chem. Soc.* **2011**, *133*, 8900.

(5) Park, K. S.; Ni, Z.; Cote, A. P.; Choi, J. Y.; Huang, R. D.; Uribe-Romo, F. J.; Chae, H. K.; O'Keeffe, M.; Yaghi, O. M. *Proc. Natl. Acad. Sci. U. S. A.* **2006**, *103*, 10186.

(6) Banerjee, R.; Phan, A.; Wang, B.; Knobler, C.; Furukawa, H.; O'Keeffe, M.; Yaghi, O. M. *Science* **2008**, *319*, 939.

(7) Wang, B.; Cote, A. P.; Furukawa, H.; O'Keeffe, M.; Yaghi, O. M. *Nature* **2008**, *453*, 207.

(8) Wang, F.; Tan, Y. X.; Yang, H.; Zhang, H. X.; Kang, Y.; Zhang, J. *Chem. Commun.* **2011**, *47*, 5828.

(9) Gucuyener, C.; van den Bergh, J.; Gascon, J.; Kapteijn, F. *J. Am. Chem. Soc.* **2010**, *132*, 17704.

(10) Wu, H.; Zhou, W.; Yildirim, T. *J. Am. Chem. Soc.* **2007**, *129*, 5314.

(11) Eum, K.; Jayachandrababu, K. C.; Rashidi, F.; Zhang, K.; Leisen, J.; Graham, S.; Lively, R. P.; Chance, R. R.; Sholl, D. S.; Jones, C. W.; Nair, S. *J. Am. Chem. Soc.* **2015**, *137*, 4191.

(12) Ma, W. J.; Jiang, Q.; Yu, P.; Yang, L. F.; Mao, L. Q. *Anal. Chem.* **2013**, *85*, 7550.

(13) Lee, J.; Farha, O. K.; Roberts, J.; Scheidt, K. A.; Nguyen, S. T.; Hupp, J. T. *Chem. Soc. Rev.* **2009**, *38*, 1450.

(14) Zhang, F.; Wei, Y. Y.; Wu, X. T.; Jiang, H. Y.; Wang, W.; Li, H. X. *J. Am. Chem. Soc.* **2014**, *136*, 13963.

(15) Dey, C.; Banerjee, R. *Chem. Commun.* **2013**, *49*, 6617.

(16) Tran, U. P. N.; Le, K. K. A.; Phan, N. T. S. *ACS Catal.* **2011**, *1*, 120.

(17) Isimjan, T. T.; Kazemian, H.; Rohani, S.; Ray, A. K. *J. Mater. Chem.* **2010**, *20*, 10241.

(18) Wang, S. B.; Yao, W. S.; Lin, J. L.; Ding, Z. X.; Wang, X. C. *Angew. Chem., Int. Ed.* **2014**, *53*, 1034.

(19) Zhan, W. W.; Kuang, Q.; Zhou, J. Z.; Kong, X. J.; Xie, Z. X.; Zheng, L. S. *J. Am. Chem. Soc.* **2013**, *135*, 1926.

(20) Corma, A.; Garcia, H. *Chem. Commun.* **2004**, 1443.

(21) Lu, G.; Li, S. Z.; Guo, Z.; Farha, O. K.; Hauser, B. G.; Qi, X. Y.; Wang, Y.; Wang, X.; Han, S. Y.; Liu, X. G.; DuChene, J. S.; Zhang, H.; Zhang, Q. C.; Chen, X. D.; Ma, J.; Loo, S. C. J.; Wei, W. D.; Yang, Y. H.; Hupp, J. T.; Huo, F. W. *Nat. Chem.* **2012**, *4*, 310.

(22) Pullen, S.; Fei, H. H.; Orthaber, A.; Cohen, S. M.; Ott, S. *J. Am. Chem. Soc.* **2013**, *135*, 16997.

(23) Tsuruoka, T.; Kawasaki, H.; Nawafune, H.; Akamatsu, K. *ACS Appl. Mater. Interfaces* **2011**, *3*, 3788.

(24) Buso, D.; Nairn, K. M.; Gimona, M.; Hill, A. J.; Falcaro, P. *Chem. Mater.* **2011**, *23*, 929.

(25) Lohe, M. R.; Gedrich, K.; Freudenberg, T.; Kockrick, E.; Dellmann, T.; Kaskel, S. *Chem. Commun.* **2011**, *47*, 3075.

(26) Falcaro, P.; Hill, A. J.; Nairn, K. M.; Jasieniak, J.; Mardel, J. I.; Bastow, T. J.; Mayo, S. C.; Gimona, M.; Gomez, D.; Whitfield, H. J.; Ricco, R.; Patelli, A.; Marmiroli, B.; Amenitsch, H.; Colson, T.; Villanova, L.; Buso, D. *Nat. Commun.* **2011**, *2*, 237.

(27) Johnson, J. A.; Luo, J.; Zhang, X.; Chen, Y. S.; Morton, M. D.; Echeverria, E.; Torres, F. E.; Zhang, J. *ACS Catal.* **2015**, *5*, 5283.

(28) Laurier, K. G. M.; Vermoortele, F.; Ameloot, R.; De Vos, D. E.; Hofkens, J.; Roeffaers, M. B. J. *J. Am. Chem. Soc.* **2013**, *135*, 14488.

(29) Xia, W.; Zhu, J. H.; Guo, W. H.; An, L.; Xia, D. G.; Zou, R. Q. *J. Mater. Chem. A* **2014**, *2*, 11606.

(30) Yang, L. L.; Yu, L.; Sun, M.; Gao, C. *Catal. Commun.* **2014**, *54*, 86.

(31) Kornienko, N.; Resasco, J.; Becknell, N.; Jian, C. M.; Liu, Y. S.; Nie, K. Q.; Sun, X. H.; Guo, J. H.; Leone, S. R.; Yang, P. D. *J. Am. Chem. Soc.* **2015**, *137*, 7448.

(32) Simmance, K.; Sankar, G.; Bell, R. G.; Prestipino, C.; van Beek, W. *Phys. Chem. Chem. Phys.* **2010**, *12*, 559.

(33) Yumashev, K. V.; Denisov, I. A.; Posnov, N. N.; Kuleshov, N. V.; Moncorge, R. *J. Alloys Compd.* **2002**, *341*, 366.

(34) Trujillano, R.; Villain, F.; Louis, C.; Lambert, J. F. *J. Phys. Chem. C* **2007**, *111*, 7152.

(35) Cappel, U. B.; Feldt, S. M.; Schoneboom, J.; Hagfeldt, A.; Boschloo, G. *J. Am. Chem. Soc.* **2010**, *132*, 9096.

(36) Klimov, V. I. *J. Phys. Chem. B* **2000**, *104*, 6112.

(37) Ludwig, J.; An, L.; Pattengale, B.; Kong, Q. Y.; Zhang, X. Y.; Xi, P. X.; Huang, J. E. *J. Phys. Chem. Lett.* **2015**, *6*, 2671.

(38) Bressler, C.; Chergui, M. *Chem. Rev.* **2004**, *104*, 1781.

(39) Chen, L. X. *Annu. Rev. Phys. Chem.* **2005**, *56*, 221.

(40) Sarangi, R.; Cho, J.; Nam, W.; Solomon, E. I. *Inorg. Chem.* **2011**, *50*, 614.

(41) Canton, S. E.; Zhang, X. Y.; Zhang, J. X.; van Driel, T. B.; Kjaer, K. S.; Haldrup, K.; Chabera, P.; Harlang, T.; Suarez-Alcantara, K.; Liu, Y. Z.; Perez, J.; Bordage, A.; Papai, M.; Vanko, G.; Jennings, G.; Kurtz, C. A.; Rovezzi, M.; Glatzel, P.; Smolentsev, G.; Uhlig, J.; Dohn, A. O.; Christensen, M.; Galler, A.; Gawelda, W.; Bressler, C.; Lemke, H. T.; Møller, K. B.; Nielsen, M. M.; Lomoth, R.; Warnmark, K.; Sundstrom, V. *J. Phys. Chem. Lett.* **2013**, *4*, 1972.

DOI: 10.1021/jacs.6b04615
J. Am. Chem. Soc. 2016, 138, 8072–8075